Human Molecular Genetics, 2014, Vol. 23, No. 9 **2251–2265**
doi:10.1093/hmg/ddt615
Advance Access published on December 2, 2013

FTY720 (fingolimod) is a neuroprotective and disease-modifying agent in cellular and mouse models of Huntington disease

Alba Di Pardo[1], Enrico Amico[1], Mariagrazia Favellato[1], Roberta Castrataro[1], Sergio Fucile[1,2], Ferdinando Squitieri[1,*] and Vittorio Maglione[1,*]

[1]IRCCS Neuromed, 86077 Pozzilli (IS), Italy and [2]Department of Physiology and Pharmacology, 'Sapienza' University of Rome, 00185 Rome, Italy

Received October 17, 2013; Revised and Accepted November 28, 2013

Huntington disease (HD) is a genetic neurodegenerative disorder for which there is currently no cure and no way to stop or even slow the brain changes it causes. In the present study, we aimed to investigate whether FTY720, the *first* approved *oral* therapy for multiple sclerosis, may be effective in HD models and eventually constitute an alternative therapeutic approach for the treatment of the disease. Here, we utilized preclinical target validation paradigms and examined the *in vivo* efficacy of chronic administration of FTY720 in R6/2 HD mouse model. Our findings indicate that FTY720 improved motor function, prolonged survival and reduced brain atrophy in R6/2 mice. The beneficial effect of FTY720 administration was associated with a significant strengthening of neuronal activity and connectivity and, with reduction of mutant huntingtin aggregates, and it was also paralleled by increased phosphorylation of mutant huntingtin at serine 13/16 residues that are predicted to attenuate protein toxicity.

INTRODUCTION

Huntington disease (HD) is an inherited brain disorder characterized by progressive degeneration of striatum and cortex and associated functional impairments in motor, cognitive and psychiatric domains (1). The disease is caused by abnormal expansion of CAG trinucleotide repeat encoding expanded polyglutamine (polyQ) stretch in the huntingtin (Htt) protein (2). Mutant Htt (mHtt) has detrimental effects on cell survival and neuronal cell functions such as synaptic transmission, gene transcription and production of a number of neurotrophins including the cortical brain-derived neurotrophic factor (BDNF) (3). The presence of the expanded polyQ stretch alters Htt structure and triggers the formation of mutant protein aggregates, thereby leading to cytotoxicity and interfering with overall cell functions (4). The expression of mutant protein has been also associated with deeply deregulated lipid metabolism, including sphingolipids breakdown (5).

FTY720, currently accepted for the treatment of relapsing remittent multiple sclerosis (6,7), is a synthetic analog of sphingosine, one of the major constituents of sphingolipids. Sphingosine is normally converted to sphingosine-1-phosphate (S1P) by sphingosine kinase-1 and -2 (SPHK1 and 2) (8). S1P is a potent signaling lipid that regulates a number of processes essential for cellular homeostasis, differentiation, motility and cell viability (8,9). Its action is mediated by the binding at S1P receptors ($S1PRs_{1-5}$), normally expressed in neurons, astrocytes and oligodendrocytes (10). The pro-drug FTY720 is able to cross the blood–brain barrier (BBB) and distributes to the brain (11), where is reversibly phosphorylated to FTY720-phosphate (FTY720-P) by endogenous SPHK2 (12). FTY720-P acts as a potent agonist at four of the sphingosine-1-phosphate (S1P) receptors ($S1P_1$, $S1P_3$, $S1P_4$ and $S1P_5$) (10,13).

FTY720 normally acts as an immuno-modulator; however, in the central nervous system (CNS), it may have a number of additional effects (14). It has been previously described to induce the activation of mitogen-activated protein kinases (MAPK) in cultured astrocytes (15), to stimulate survival of oligodendrocyte progenitors through the activation of AKT and ERK pathways (16) and to protect cultured cortical neurons by increasing

*To whom correspondence should be addressed at: Centre for Neurogenetics and Rare Diseases, IRCCS Neuromed, Localita' Camerelle, 86077 Pozzilli (IS), Italy. Tel: +39 0865915250; Fax: +39 0865927575; Email: vittorio.maglione@neuromed.it (V.M.); Tel: +39 0865 915248; Fax: +39 0865 927575; Email: ferdinando.squitieri@lirh.it (F.S.)

BDNF production (17) and reducing NMDA-mediated excitotoxicity (18). Administration of FTY720 has been recently reported to increase BDNF levels and significantly prolong survival in a mouse model of Rett syndrome (19), suggesting a potential therapeutic of FTY720 for the treatment of brain disorders, other than MS.

In the present study, we investigated whether FTY720 might be effective in HD models. Our findings indicate that chronic administration of FTY720 leads to improved motor function, prolonged survival and reduced brain atrophy in HD R6/2 mice. Remarkably, the benefits of the treatment were associated with increased BDNF levels, strengthening of neuronal activity and connectivity and reduction of mHtt aggregates. Interestingly, FTY720 treatment evoked phosphorylation of mutant huntingtin at serine 13/16 residues both *in vitro* and *in vivo*.

RESULTS

Administration of FTY720 protects HD cell model from apoptosis and promotes phosphorylation of pro-survival molecules, AKT and ERK

Striatal-derived cell line expressing endogenous levels of mHtt ($STHdh^{111/111}$) showed higher susceptibility to apoptosis when compared with wild-type Htt-expressing cells ($STHdh^{7/7}$) (5). First, to test the hypothesis that FTY720 was able to protect HD cells from apoptosis, $STHdh^{7/7}$ and $STHdh^{111/111}$ were grown in serum-free medium for 8 h in the presence of 1 μM FTY720. Administration of the pro-drug significantly reduced apoptosis in both cell lines (Fig. 1A) and rapidly induced phosphorylation of either AKT or ERK (Fig. 1B and C).

The neuroprotective effect of FTY720 is mimicked by FTY720-P and other S1P receptor agonists and is partially due to sphingosine kinase 2 activity

To explore additional molecular mechanism behind the neuroprotective effect of FTY720, we tested the involvement of S1PRs. A number of evidence demonstrates that stimulation of such receptors may exert anti-apoptotic effects in different cell death paradigm (20,21). First, to address the question whether a direct stimulation of S1PRs was neuroprotective also in HD models, $STHdh^{111/111}$ cells were cultured in serum-free medium in the presence of different S1P receptor agonists: S1P, FTY720-P and SEW2871. Our results showed that all the S1PR agonists used efficiently reduced apoptosis in HD cell lines (Fig. 2A–C).

Next, in attempt to explore whether the neuroprotective effects of FTY720 were exclusively attributable to its active form FTY720-P, we co-treated HD cells with 1 μM FTY720 and 10 μM SPHKs inhibitor, D-erythro-*N*,*N*-dimethylsphingosine (22). SPHK2 mediates the conversion of the pro-drug FTY720 to the active form FTY720-P (12,13). DMS treatment failed to completely block the anti-apoptotic action of FTY720 (Fig. 2D), indicating that FTY720-mediated neuroprotection was partially dependent on the conversion of FTY720 to FTY720-P.

Infusion of FTY720 improves motor functions and prolongs lifespan in R6/2 mice

In order to test the hypothesis that FTY720 may exert beneficial effect *in vivo* in HD, R6/2 mice at different weeks of age and wild-type littermate controls were daily i.p.- injected with FTY720 or vehicle. Seven- and 10-week-old mice were treated in order to assess the effect of FTY720 on motor performance and lifespan (Figs 3 and 4). Motor function was analyzed before and at fixed time points (once a week) during the treatment. In line with previous studies, at the time when the treatment with FTY720 was initiated, 7- and 10-week-old R6/2 mice showed severe motor impairment compared with WT littermates (23), as assessed by open-field and horizontal ladder task (Fig. 3A–C). Remarkably, the beneficial effects of the compound on motor function and coordination were observed after 1 week of treatment (Fig. 3A–C). FTY720 chronically infused-R6/2 mice performed significantly better than vehicle-treated mice during the whole period of the treatment (Fig. 3A–C). No effects on motor behavior were observed in WT mice. According to the Kaplan–Meyer survival curve, both groups of FTY720-treated R6/2 mice (7- and 10-week-old mice) showed an extended survival compared with the vehicle groups (Fig. 4A and B). Furthermore, FTY720 treatment preserved HD mice from the weight loss, normally associated with the disease progression (Fig. 4C). Our results point out an overall good safety and tolerability profile of FTY720 with no evidence of adverse events throughout the period of the treatment.

FTY720 induces phosphorylation of AKT and ERK *in vivo*

Next, we explored the possibility that FTY720 was able to induce activation of pro-survival AKT and ERK also in mouse striatal tissues. To this purpose, 7-week-old vehicle- and FTY720-treated WT and R6/2 mice were sacrificed within 1 h from the last drug injection. In agreement with the results obtained *in vitro*, administration of FTY720 significantly incremented the phosphorylation levels of both AKT and ERK in either R6/2 (Fig. 5A and B) or WT mice (Fig. 5C and D), highlighting the ability of the drug to modulate the activity of 'classical effectors' of neuronal survival also *in vivo*. The increase of AKT and ERK phosphorylation, induced by FTY720 administration, appeared less pronounced in R6/2 with respect to WT brain tissues, corroborating the defects in the molecular pathways involving such kinases (24–26).

FTY720 ameliorates R6/2 mice neuropathology

Analysis of brain atrophy

The biological effect of FTY720 on neuropathology was assessed on serial brain coronal sections of whole brains from 11-week-old mice. R6/2 mice have been previously reported to progressively lose brain weight from ∼7 weeks of age (23). After the administration of FTY720, mice showed a marked reduction in brain weight loss when compared with the vehicle-treated mice (Fig. 6A). This result was associated with higher number of striatal cells as measured by hematoxylin/eosin staining (Fig. 6B) and with reduced extend of ventricle enlargement (Fig. 6C). Interestingly, semi-quantitative analyses of anatomical structure of corpus callosum (CC) revealed a significant

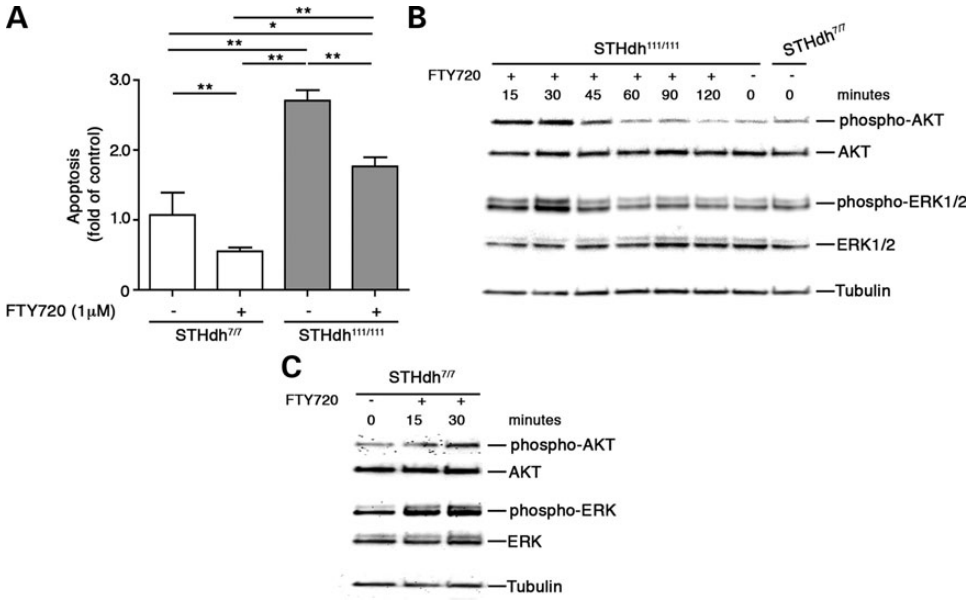

Figure 1. Administration of FTY720 protects WT and HD striatal-derived cell lines from apoptosis and results in AKT and ERK activation. (**A**) Apoptosis in striatal-derived cell lines cultured for 6 h in serum-free medium in presence or absence of 1 μM FTY720. Data are represented as mean ± SD of three experiments, each performed in triplicate. $^{*}P<0.05$; $^{**}P<0.001$ (non-parametric Mann–Whitey *U*-test). (**B** and **C**) AKT and ERK phosphorylation in cellular protein extracts in HD (B) and WT (C) striatal-derived cell lines measured at different time points after FTY720 treatment.

reduction in its thickness in R6/2 mice when compared with WT mice. Importantly, chronic infusion of FTY720 partially prevented such reduction (Fig. 6C and D) in R6/2 mice, highlighting potential disease-modifying properties of the drug. Neuropathological changes in FTY720-treated mice were also associated with higher levels of striatal dopamine- and cAMP-regulated protein 32 (DARPP-32), a specific marker of medium spiny neurons (Fig. 6E), and increased levels of myelin–associated glycoprotein (MAG), a marker of myelin and white matter (WM) integrity (27), when compared with vehicle-treated mice (Fig. 6F). DARPP-32 protein levels were also increased in WT striatal tissues (Supplementary Material, Fig. S1), further confirming the potential ability of the drug to reinforce neuronal activity independently of the pathological condition.

Analysis of mutant huntingtin aggregates in R6/2 brain

To investigate the possibility that FTY720 may lower Htt toxicity, we evaluated its effect on mHtt aggregation. Formation of mHtt aggregates is a pathological hallmark that may conceivably cause neuronal dysfunction in HD (28). Immunohistochemical analysis using EM48 antibody revealed a dramatic reduction of either number or area of mHtt aggregates in the striatum of 11-week-old FTY720-treated R6/2 mice compared with controls (Fig. 6G–I).

FTY720 increases BDNF brain levels

In line with previous evidence highlighting the ability of FTY720 to promote elevation of BDNF both *in vitro* and *in vivo* (19), we found a significant increase of cortical BDNF mRNA levels both in R6/2 and WT treated mice (Fig. 7A). Consistently, BDNF protein levels were found elevated in the cortical tissues of FTY720-treated R6/2 mice (Fig. 7B and C) as well as in the striatum of the same mice, suggesting FTY720 to be potentially able to ameliorate the anterograde transport of the neurotrophin in R6/2 mice and supporting the hypothesis of a possible improvement of overall cortical-striatal transmission after the treatment.

FTY720 ameliorates cortical neuronal activity

BDNF has been reported to revert the increased GABAergic transmission in R6/2 mice (29), and its FTY720-mediated up-regulation may likely induce recovery of cortical-striatal transmission. Thus, we analyzed the GABAergic inputs to layer IV–V cortical pyramidal neurons. Vehicle- and FTY720-treated mice were sacrificed at 8 weeks of age, and frequency and amplitude of spontaneous inhibitory post-synaptic currents (sIPSCs) were measured. Similar to previous studies (29), the sIPSCs frequency was significantly higher in R6/2 than that in WT mice (Fig. 8A and B). The sIPSCs amplitude was also significantly increased, though to a lower extent (Fig. 8C). In FTY720-treated R6/2 mice, the observed reduction in sIPSCs frequency was not significant (Fig. 8B), whereas mean amplitude was significantly lowered to WT values (Fig. 8C). To deeper investigate the cortical GABAergic transmission, we analyzed miniature inhibitory post-synaptic currents (mIPSCs), owing to the spontaneous GABA release in the tetrodotoxin (TTX)-induced inhibition of action potential propagation. The mIPSCs frequency was obviously increased in R6/2 mice (Fig. 8D and E), whereas the amplitude was similar to WT values (Fig. 8F). Confirming the analysis of sIPSCs, the FTY720 treatment significantly reduced mIPSCs amplitude in R6/2 mice (Fig. 8F), leaving unaffected their frequency (Fig. 8E). These results indicated a clear FTY720-induced functional action on GABAergic synapses impinging cortical pyramidal neurons, with a partial but significant recovery of inhibitory transmission to physiological conditions.

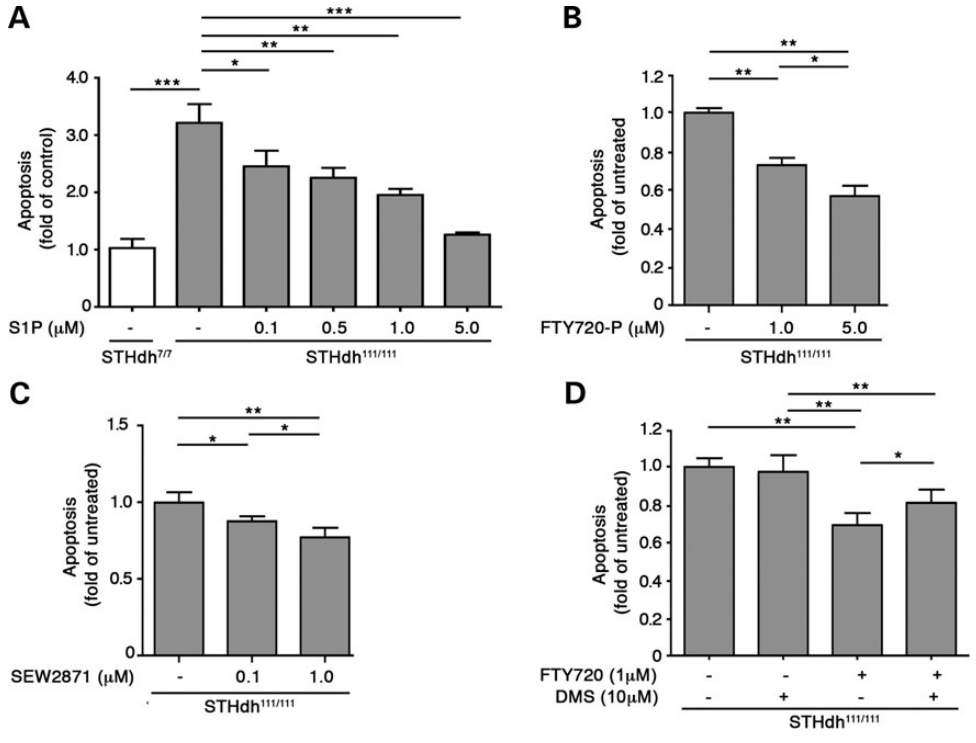

Figure 2. The neuroprotective effect of FTY720 is mimicked by different S1P receptor agonists and is partially dependent on its phosphorylated form. Apoptosis in striatal-derived cell lines cultured for 6 h in serum-free medium in presence or absence of different concentrations of S1PRs agonists: S1P (**A**), FTY720-P (**B**) and SEW2871 (**C**). (**D**) Apoptosis in STHdh$^{111/111}$ cell lines cultured for 6 h in serum-free medium in presence or absence of 1 μM FTY720 and/or 10 μM sphingosine kinases inhibitor, DMS. Data are represented as the mean ± SD of three experiments, each performed in triplicate. $^{*}P < 0.05$; $^{**}P < 0.001$; $^{***}P < 0.0001$ (non-parametric Mann–Whitney *U*-test).

FTY720 treatment increases endogenous GM1 levels *in vitro* and *in vivo* HD models

Evidence indicates that FTY720, but not FTY720-P, may increase levels of C18-ceramide, a natural precursor of brain sphingolipids including gangliosides (30). Defective ganglioside metabolism leads to increased susceptibility of HD cells to apoptosis, and administration of ganglioside GM1 is neuroprotective in HD models (5,31). Here, we observed that administration of FTY720 increased mRNA levels of GM1 synthase (β3galt4) and plasma membrane GM1 content in STHdh$^{111/111}$ cells (Fig. 9A and B). Similarly, GM1 levels were restored in the striatum of FTY720-treated R6/2 mice compared with vehicle-treated mice (Fig. 9C). These results would suggest a potential ability of the drug to retrieve the altered ganglioside metabolism in HD models.

FTY720 treatment induces Htt phosphorylation at serine 13/16 residues both *in vitro* and *in vivo*.

To further investigate a possible molecular event by which the drug may specifically impact HD pathophysiology, we tested the potential of FTY720 to modulate mHtt phosphorylation at serine 13/16 residues, previously reported as critical determinants in the pathogenesis of the disease (32). Administration of 1 μM FTY720 increased levels of phospho-Ser13/16 Htt in HD STHdh$^{111/111}$ cells as assessed by using the phospho-specific antibody (pN17) (31,33) (Fig. 10A–C). Phosphorylated huntingtin migrated at higher molecular weight than full-length Htt (FL-Htt), consistent with the formation of an SDS–insoluble protein complex which we have previously defined as high-molecular-weight huntingtin (HMW-Htt) (Fig. 10C) (31). Similar result was observed in R6/2 striatal lysates, where only the HMW-Htt complex was detected by pN17 (Supplementary Material, Fig. S2).

DISCUSSION

FTY720, a Food and Drug Administration (FDA)-approved oral agent for the treatment of MS, was first described as an immunosuppressive drug (34) and recently reported to have neuroprotective and neurorestorative properties (18,19,35) that make FTY720 a potential therapeutic drug for treatment of different neurodegenerative disorders (19). In this study, we evaluated whether FTY720 may represent a possible pharmacological intervention also in HD.

FTY720 significantly reduced apoptosis in STHdh cell models and evoked pro-survival pathways responses by inducing activation of AKT and ERK. This is particularly important in the context of HD where PI3 /AKT and ERK pathways are notoriously impaired (24–26) and stimulation of each of these molecules is reported to be beneficial (5,36–38). The efficacy of FTY720 may depend on the stimulation of S1PRs by its phosphorylated form (FTY720-P) (13). Coherently, stimulation of such receptors is neuroprotective in HD striatal cell lines and suggests that the direct stimulation of S1PRs may be considered as potential target for new therapeutic strategies for the disease.

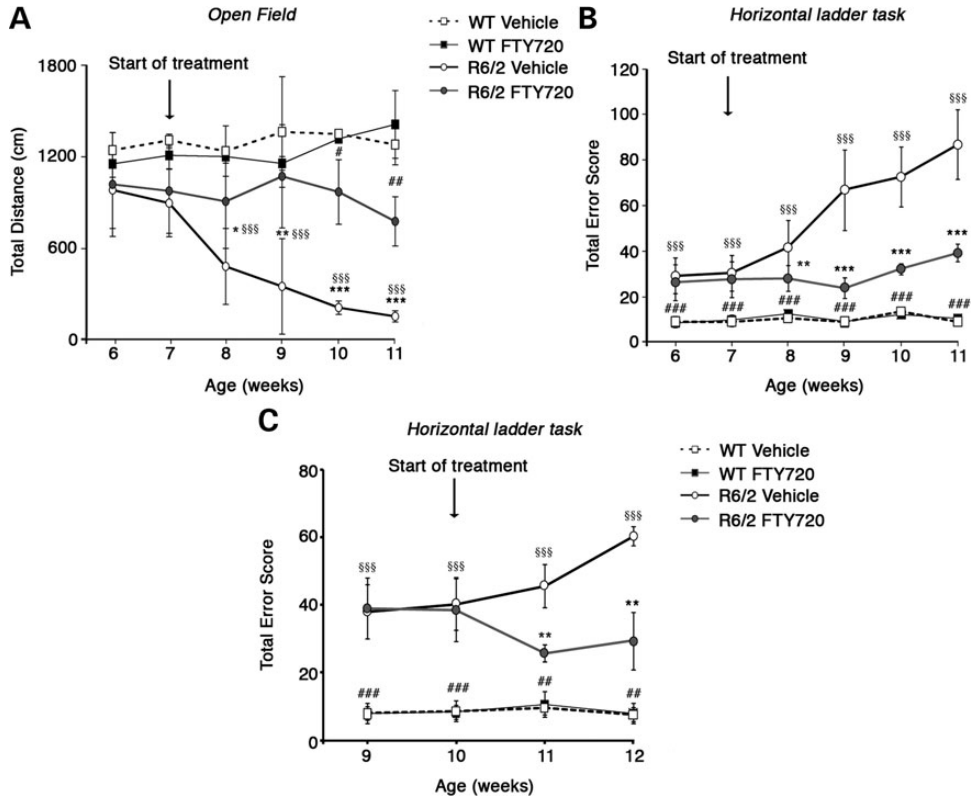

Figure 3. Chronic administration of FTY720 (0.1 mg/kg) improves motor function in R6/2 mice. (**A**) General locomotor activity in the open field in 7-week-old R6/2 mice and control littermates, before and after treatment. (**B**) Analysis of motor coordination on horizontal ladder task before and after the treatment in 7-week-old or (**C**) 10-week-old mice. Each data point represents the average performance ± SD of 8–10 mice for each group of mice. $^{*}P < 0.05$; $^{**}P < 0.001$; $^{***}P < 0.0001$ (FTY720-treated R6/2 versus vehicle-treated R6/2); $\#P < 0.05$; $\#\#P < 0.001$; $\#\#\#P < 0.0001$ (vehicle- and FTY720-treated WT versus FTY720-treated R6/2); §§§$P < 0.0001$ (vehicle- and FTY720-treated WT versus vehicle-treated R6/2; two-way ANOVA with Bonferroni post-test).

On the other hand, the pharmacological inhibition of the conversion of FTY720 to FTY720-P, by DMS, failed to completely block the anti-apoptotic properties of the drug in HD, indicating that FTY720-P may not be the only effective form.

Starting from the first week and throughout the duration of the treatment, FTY720-treated R6/2 mice performed significantly better than their controls. The progression of the disease was dramatically slowed down up to the animal death that was significantly delayed independently of the age at which animal underwent the treatment. Interestingly, the efficacy of FTY720 on motor symptoms, even at very late stages of the disease, pointed out an important therapeutic potential of the molecule in HD. Recovery of motor function and overall wellbeing of FTY720-treated R6/2 mice well correlated with reduced loss of brain weight limited ventricles enlargement and higher number of striatal cells probably including neuronal and non-neuronal cell populations (e.g. oligodendrocytes) (14,16). Neuropathological improvements were associated with increased levels of DARPP-32 protein, whose defective expression is an early sign of striatal dysfunction and neuronal loss in R6/2 (39). Increased levels of DARPP-32 in HD mice, after FTY720, may be due to reduced loss of striatal neurons. FTY720 may preserve medium spiny neuronal function and protect these neurons from degeneration. This effect may likely reinforce cell signaling and eventually correlate with an improved neuronal activity.

FTY720 mediates tissues remodeling processes and normally distributes in CNS WM preferentially along myelin sheaths (40), leading to attenuated injury to oligodendrocytes, myelin and axons in the CC of mice with chemical-induced WM damage (41). WM segmentation and myelin breakdown is described in different HD mouse models at different stages of the disease (42,43).

In this study, FTY720 significantly reduced the thinning of CC and restored levels of MAG protein, which normally localizes in periaxonal Schwann cells and oligodendroglial membranes of myelin sheaths, where it regulates signaling and stabilizes glia–axon interactions (27) as well as WM integrity (44). MAG-null phenotype results in loss of axonal neurons and increased susceptibility to excitotoxic stimuli and seizure activity (45,46). Restoring levels of MAG may likely stabilize axonal–glial interactions and preserve neuronal function and survival in HD.

The beneficial effects of FTY720 on HD striatum and CC neuropathology might be the result of a direct action of the drug on the two distinct regions or secondary to the effectiveness of the drug to specifically increase the levels of BDNF protein, as this neurotrophin has been reported to regulate the expression of DARPP-32 and MAG in medium spiny neurons and WM, respectively (47,48). BDNF is normally synthesized in the cortex and transported to the striatum via cortico-striatal projections and provides the main support for survival of striatal

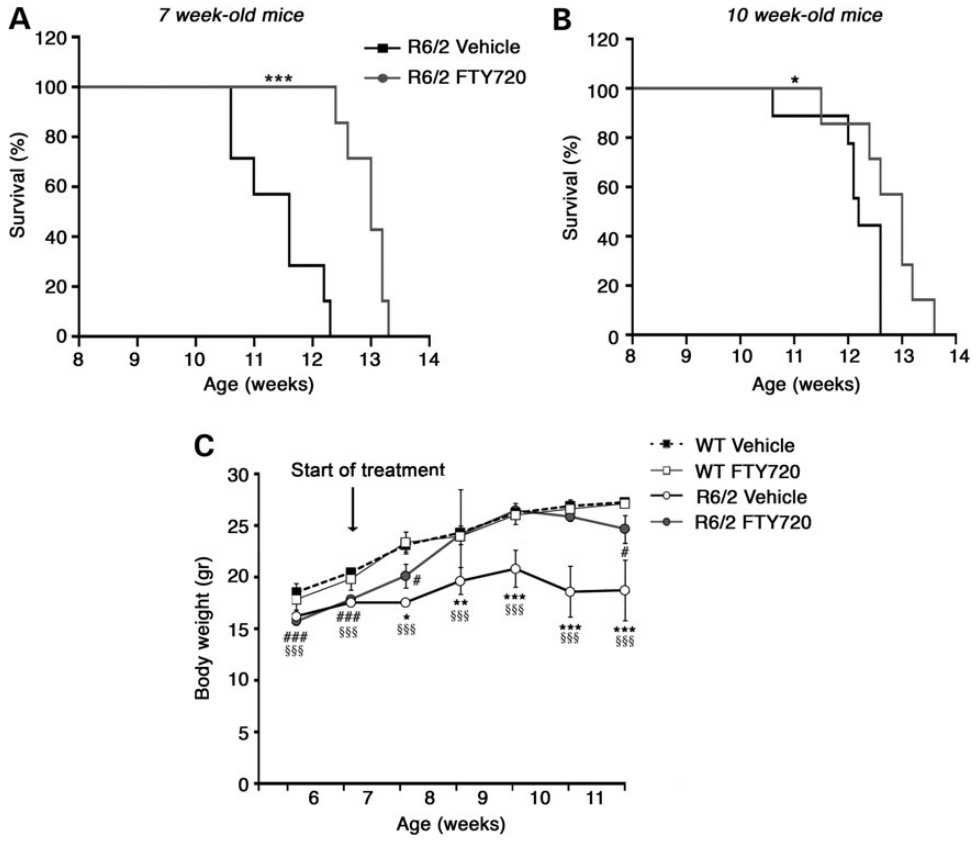

Figure 4. FTY720 prolongs lifespan and stabilize body weight in R6/2 mice. (**A**) Kaplan–Meier probability of survival analysis in FTY720- and vehicle-treated R6/2 mice at 7 weeks of age, $n = 7–8$ for each group of mice. $^{***}P < 0.001$ (log-rank test), median survival ratio (untreated versus treated): 0.8923; hazard ratio (untreated versus treated): 4.620. (**B**) Kaplan–Meier probability of survival analysis in FTY720- and vehicle-treated R6/2 mice at 10 weeks of age of age, $n = 7–8$ for each group of mice. $^{*}P < 0.05$ (Log-rank Test); median survival ratio (untreated versus treated): 0.9385; hazard ratio (untreated versus treated): 2.248. (**C**) Analysis of mouse body weight in all groups of animal. Each data point represents the average of body weight ± SD of 10 mice. $^{*}P < 0.05$; $^{***}P < 0.0001$ (FTY720-treated R6/2 versus vehicle-treated R6/2); $^{\#}P < 0.05$, $^{\#}P < 0.0001$ (vehicle- and FTY720-treated WT versus FTY720-treated R6/2); $^{§§§}P < 0.0001$ (vehicle- and FTY720-treated WT versus vehicle-treated R6/2; two-way ANOVA with Bonferroni post-test).

neurons in the adult brain (49). Reduced levels of BDNF, altered gene expression and/or abnormalities in its anterograde transport in cortical regions have been previously implicated in the pathogenesis of HD (3,50). Administration of FTY720 increased BDNF levels in both WT and HD mice. Although this effect was independent of the mouse genotype, increased levels of BDNF in HD mouse cortex and the restoration in the striatum of same mice suggest FTY720 as a modulator of BDNF expression and release in HD and rises the hypothesis that the neuroprotective effect of the drug may also be mediated by the neurotrophin, as BDNF prevents loss of striatal neurons and motor dysfunction in HD mouse models (51,52). HD mice, including R6/2, display a progressive impairment in both excitatory and inhibitory synaptic transmission, in both striatum and cortex (53). In particular, GABAergic inputs are functionally enhanced in the first stages of the pathology and then strongly decreased, likely due to interneuron death in the last period of R6/2 mice life (29). Here we found that FTY720 partially but significantly reduced GABAergic transmission in the cortices of 8-week-old R6/2 mice, making their fast inhibitory signaling similar to that of WT animals. This effect is likely to be mediated by FTY720-induced BDNF production, as this neurotrophin has been also shown to revert the increased GABAergic function in the striatum (29).

An important finding of our study is the dramatic reduction of mHtt aggregates of FTY720-treated R6/2 mice. Although it is still unclear whether aggregates are the toxic Htt species (54), their reduction is often associated with an improvement of disease phenotype in different HD models (55).

The pro-drug FTY720 has been previously demonstrated to have an intrinsic activity to influence lipids homeostasis (30,56). Disrupted metabolism of lipids, in particular gangliosides, has been described as critical determinant of HD pathogenesis (5). Administration of exogenous GM1 restored normal levels of ganglioside in HD cellular and animal models, and it resulted to be beneficial both *in vitro* and *in vivo* (5,31). Here, we reported that FTY720 modulated endogenous GM1 levels in $STHdh^{111/111}$ cells and restored its normal content also in the striatum of R6/2 mice. Thus, the effect of FTY720 on gangliosides metabolism may reinforce its neuroprotective function in HD models and further contribute to the amelioration of the pathology.

Phosphorylation of Htt at serine 13/16 residues is reported to have several beneficial effects in HD models by changing mHtt

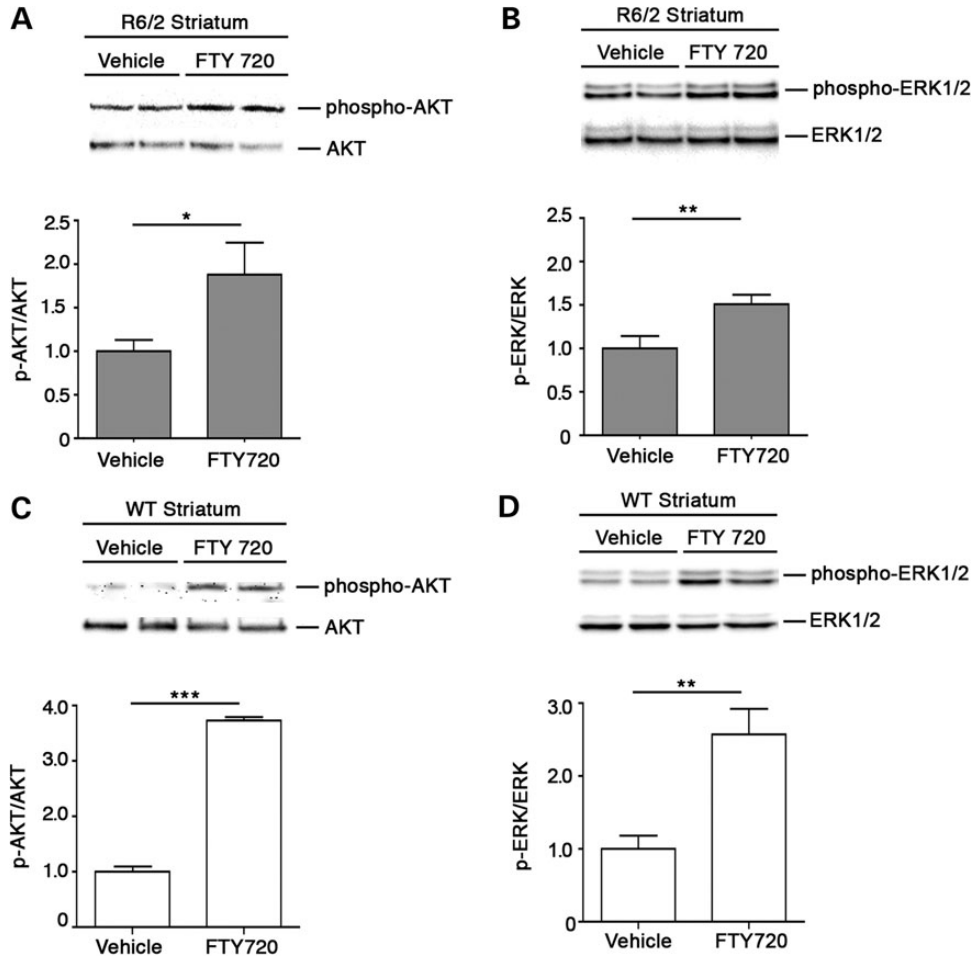

Figure 5. FTY720 induces AKT and ERK phosphorylation *in vivo*. Representative western blottings and densitometric analysis of AKT and ERK phosphorylation in striatal tissues from R6/2 (**A** and **B**) and WT mice (**C** and **D**) after acute infusion of FTY720 (0.1 mg/kg). Data are represented as mean ± SD, $n = 5$ for each group of mice. $^{*}P < 0.05$; $^{**}P < 0.001$; $^{***}P < 0.0001$ (non-parametric Mann–Whitney *U*-test).

conformation (33,57), reducing mutant Htt exon1 aggregation and toxicity (58) and by increasing mutant protein degradation (59). Importantly, in BACHD mice expressing Ser13 and Ser16 phosphomimic mHtt, behavioral features of the disease, including motor and psychiatric deficits, are significantly ameliorated and mHtt aggregates in the brain are not detected (32). In this study, we reported the evidence that FTY720 triggered Htt phosphorylation at serine 13/16 residues both *in vitro* and *in vivo*. In line with our previous findings (31), we were able to detect phosphorylation at serines 13 and 16 only in the HMW-Htt and not in the FL-Htt. These results corroborated the hypothesis that phosphorylation of Htt at such serine residues may be involved in the stabilization and/or formation of HMW-Htt complex (31) whose nature is not fully determined yet. HMW-Htt could represent mHtt aggregates species (60), and the increased phosphorylation state may appoint them to degradation (59), thus explaining the reduction of mHtt inclusions in R6/2 striatum.

Although in this study, there is no prove of a direct correlation between increased levels of phospho-mHtt and the neuroprotective effect of the drug, we believe that compounds like FTY720, which cross the BBB and promote all the beneficial effects we described, may likely result effective for treating the disease. To our best knowledge, this is the first evidence of a compound exerting neuroprotective action to such extent in HD models.

We believe that the pre-clinical efficacy of FTY720 reported in this study highlights the therapeutic potential of the drug to treat HD. What might make FTY720 superior to other drugs is the fact that, beside its ability to improve motor function and neuropathology in R6/2 mice, which would make it an effective disease-modifying drug in HD, it has the potential of impacting critical disease-related deficits. Neuroprotective and neurorestorative proprieties of the drug, as well as the safety profile observed in R6/2 mice and, importantly, also in clinical trials for other neurological disorders (61), indicate that FTY720 may represent a valuable and alternative therapeutic approach that can be transferred into clinical practice in HD in the next future.

MATERIALS AND METHODS

Chemicals

FTY720, FTY720-phosphate (FTY720-P), 1,2,4-oxadiazole, 5-[4-phenyl-5-(trifluoromethyl)-2-thienyl]-3-[3-(trifluoromethyl)

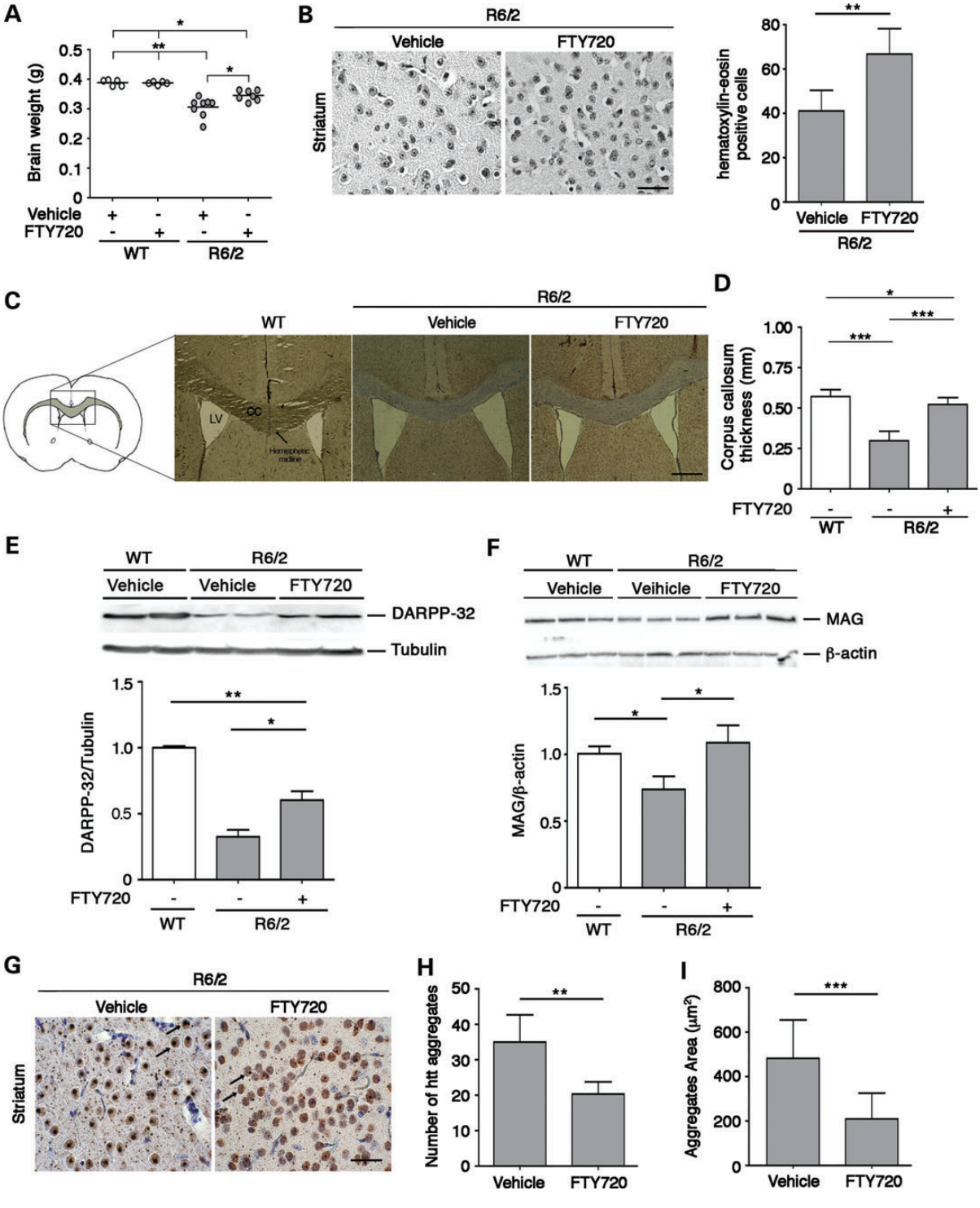

Figure 6. FTY720 ameliorates R6/2 neuropathology. (**A**) Average brain weight of 11-week-old vehicle- and FY720-treated WT and R6/2 mice, vehicle- and FTY-treated WT mice, $n = 5$ for each group; vehicle-treated R6/2 mice, $n = 8$; FTY720-treated mice, $n = 7$, $^{*}P < 0.05$; $^{**}P < 0.001$ (non-parametric Mann–Whitey *U*-test). (**B**) Representative hematoxylin/eosin staining in striatal tissues from vehicle- and FTY720-treated R6/2 mice at 11 weeks of age (scale bar: 25 μm). Graph represents the quantitation of hematoxylin/eosin-positive cells, $n = 5$ for each group of mice. (**C**) Representative micrograph of CC thickness and ventricle enlargement in WT (left), vehicle- (center) and FTY720-treated R6/2 (right) mice (scale bar: 200 μm). LV: lateral ventricle. (**D**) CC thickness (mm) in correspondence of the middle line of the brain as indicated in (**C**). (**E**) Representative western blotting and densitometric analysis of DARPP-32 protein levels in the striatum of vehicle- and FTY720-treated mice at 11 weeks of age. Data are represented as mean ± SD, $n = 5$ for each group of mice. $^{*}P < 0.05$; $^{**}P < 0.001$ (non-parametric Mann–Whitey *U*-test). (**F**) Representative western blotting and densitometric analysis of MAG in WM in the same group of animals. Data are represented as mean ± SD, $n = 5$ for each group of mice. $^{*}P < 0.05$ (non-parametric Mann–Whitey *U*-test). (**G**) Representative micrograph of EM48-positive striatal mHtt aggregates from vehicle- and FTY720-treated R6/2 mice at 11 weeks of age. Arrows indicate mHtt aggregates (scale bar: 25 μm). (**H** and **I**) Semi-quantitative analysis of both number and area of mHtt aggregates. Data are represented as mean ± SD, $n = 5$ for each group of mice. $^{**}P < 0.001$; $^{***}P < 0.0001$ (two-tailed *t*-test).

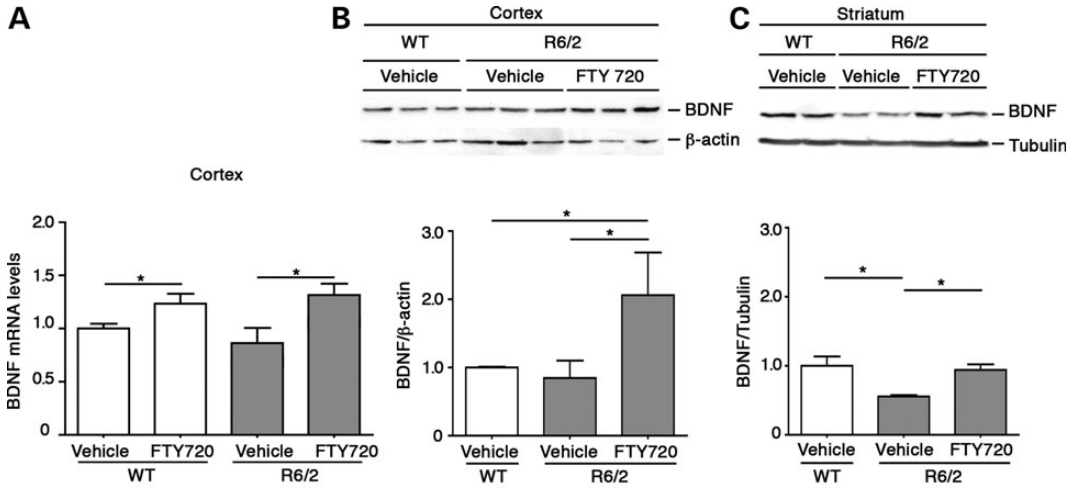

Figure 7. FTY720 increases BDNF levels in cortex and striatum. (**A**) BDNF mRNA levels in cortical tissues from 11-week-old vehicle- and FTY720-treated mice. Data are represented as mean ± SD, $n = 5$ for each group of mice. $^{*}P < 0.05$ (non-parametric Mann–Whitney *U*-test). (**B**) Representative western blotting and densitometric analysis of BDNF protein in cortical tissues from vehicle- and FTY720-treated mice at 11 weeks of age. (**C**) Representative western blotting and densitometric analysis of BDNF protein expression in the striatum of the same group of mice. Data are represented as mean ± SD, $n = 5$ for each group of mice. $^{*}P < 0.05$ (non-parametric Mann–Whitney *U*-test).

phenyl] (SEW2871) were purchased from Santa Cruz. D-Erythro-*N*,*N*-dimethylsphingosine was purchased from ENZO Life Sciences. All chemicals were dissolved according to the manufacturer's instructions.

Cell models

Conditionally immortalized mouse striatal knock-in cells expressing endogenous levels of wild-type ($STHdh^{7/7}$) or mHtt ($STHdh^{111/111}$) were purchased from the Coriell Cell Repositories (Coriell Institute for Medical Research, Camden, NJ, USA) and were maintained as previously described (5).

Lysates preparation

After pre-incubation for 5 h at 33°C in serum-free medium, cells were treated with 1 μM FTY720 for the indicated time. Cells were lysate in lysis buffer containing 20 mM Tris, pH 7.4, 1% Nonidet P-40, 1 mM EDTA, 20 mM NaF, 2 mM Na_3VO_4 and 1:1000 protease inhibitor mixture (Sigma–Aldrich), sonicated with 2 × 10 s pulses and then centrifuged for 10 min at 10 000*g*.

Analysis of apoptosis

The–anti-apoptotic effect of FTY720, FTY720-P, SEW2871 and S1P was tested on immortalized cells cultured in serum-free medium at 39°C at the indicated time in the presence of the specific compound. In FTY720 experiments, cells were pre-incubated with FTY720 for 2 h before they were placed at 39°C. In DMS experiments, cells were pre-incubated with DMS for 1 h before adding FTY720. At the end of each treatment, cells were collected and incubated with FITC-conjugated Annexin V (Southern Biotech) according to the manufacturer's instructions. Fluorescence-activated cell sorting (FACS) analysis was performed as previously described (5).

Animal models

Breeding pairs of the R6/2 line of transgenic mice [strain name: B6CBA-tgN (HDexon1) 62Gpb/1J] with ∼160 ± 10 (CAG) repeat expansions were purchased from the Jackson Laboratories (Bar Harbor, ME, USA) and maintained in the animal facility at IRCCS Neuromed. *In vivo* experiments were approved by IRCCS Neuromed and carried out in both R6/2 mice and WT littermates, starting from 5 or 10 weeks of age. To ensure homogeneity of experimental cohorts, mice from the same F generation were assigned to experimental groups, such that age and weight were balanced. In total, 64 male R6/2 transgenic mice and 50 male WT littermates were used in this study. All animals used for biochemical and histological experiments were euthanized at fixed time points. R6/2 mice used for testing the effect of FTY720 on mouse survival died naturally.

Protein lysate preparation

Mice were sacrificed by cervical dislocation, brain regions were dissected out, snap-frozen in liquid N2 and pulverized in a mortar with a pestle. Pulverized tissue was homogenized in lysis buffer containing 20 mM Tris, pH 7.4, 1% Nonidet P-40, 1 mM EDTA, 20 mM NaF, 2 mM Na_3VO_4 and 1:1000 protease inhibitor mixture (Sigma–Aldrich), sonicated with 2 × 10 s pulses and then centrifuged for 10 min at 10 000*g*.

Immunoblottings

For analysis of phospho-AKT and phospho-ERK, 40 μg of total lysate was immunoblotted with the following antibodies: anti-phospho-AKT (1:1000), anti-AKT (1:1000), anti-phospho-ERK (1:1000) and anti-ERK (1:1000) (all from Cell Signaling). For DARPP-32, BDNF and MAG total lysate were immunoblotted with the following antibodies: anti-DARPP-32 (1:1000), anti-BDNF (1:500) and anti-MAG (L20) (1:1000) (all from Santa Cruz), respectively. For the analysis of huntingtin phosphorylation at serine 13/16 residues, 40 μg of striatal lysate was immunoblotted with the following antibodies: anti-phospho-Se13/16-specific antibody pN17 (1:6000) (31,33) and anti-Huntingtin N17 (1:6000) (31,33). For protein normalization, anti-α tubulin (1:5000) (Abcam) or anti-β Actin (1:3000) (Sigma) was used.

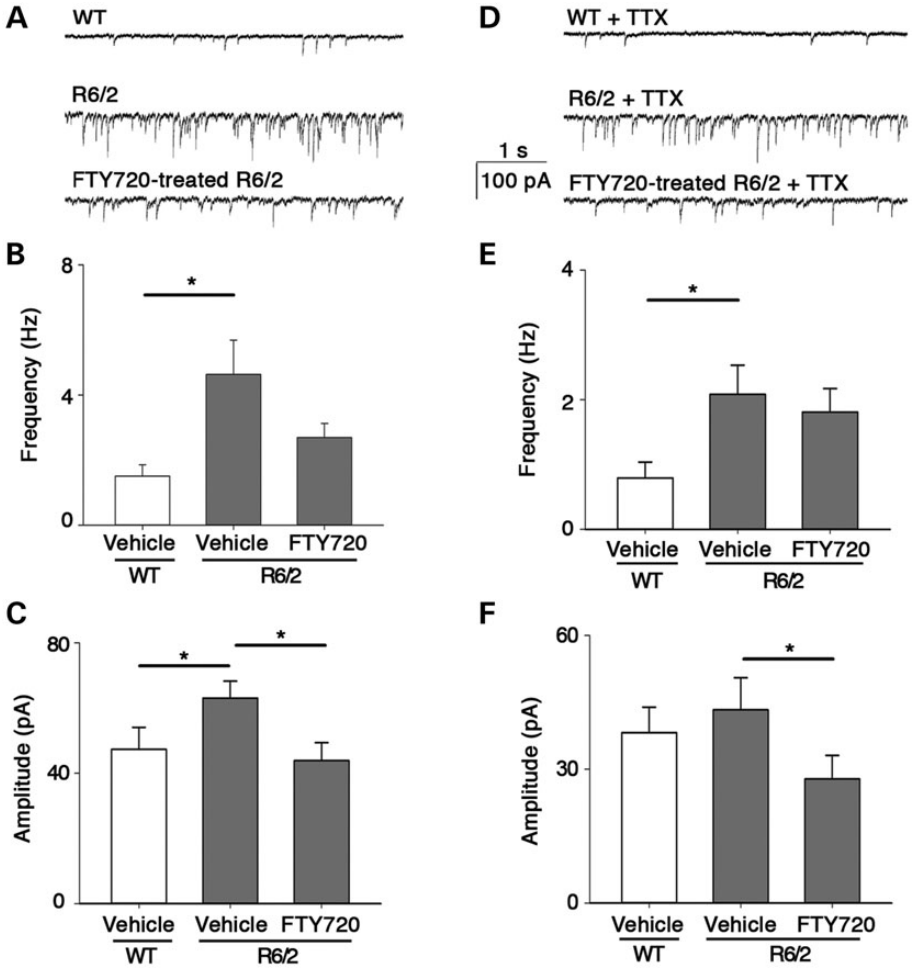

Figure 8. FTY720 restores GABAergic synaptic transmission in 8-week-old R6/2 mice to physiological levels. (**A**) Typical whole-cell recording from layer IV–V pyramidal neurons in slices from WT (top), R6/2 (middle) and FTY720-tretaed (bottom) mice. (**B**) Histogram of sIPSCs mean frequency, same conditions as (A), $n = 10$ for each bar. (**C**) Histogram of sIPSCs mean amplitude, same cells as (B). (**D**) Typical whole-cell recording from neurons in slices from WT (top), R6/2 (middle) and FTY720-treated (bottom) mice in the presence of TTX 1 μM; other conditions as in (A). (**E**) Histogram of mIPSCs mean frequency, same conditions as (D), $n = 10$ for each bar. (**F**) Histogram of mIPSCs mean amplitude, same cells as (E). Data are expressed as mean ± SEM; $^{*}P < 0.05$ (non-parametric Mann–Whitney *U*-test). Holding potential −70 mV; CNQX 10 μM, AP-5 50 μM.

HRP-conjugated secondary antibodies (GE Healthcare) were used at 1:5000 dilution. Protein bands were detected by ECL Prime (GE Healthcare) and quantitated with Quantity One (Bio-Rad Laboratories) and/or ImageJ software.

In vivo drug administration

FTY720 was dissolved in DMSO according to the manufactory instructions and daily administered by intraperitoneal (i.p.) injection at dose of 0.1 mg/kg of body weight according to Deogracias *et al*. (19). FTY720 solution was further dissolved in saline (vehicle). Control mice (WT and R6/2) were daily injected with the same volume of vehicle containing DMSO.

Motor behavior tests and survival study

Open-field test and horizontal ladder task were performed according to the standard recommendations. All tests took place during the light phase of the light–dark cycle. Male mice were first habituated to the test room and to the instrument and task to perform for 2 h before any test. Spontaneous horizontal locomotion and general motor activity were analyzed in the open field. Mice were placed in the center of the chamber, and their behavior was recorded for 5 min. Quantitative analyses were performed on the total distance traveled. Skilled walking, limb placement and limb coordination were all assessed by the ladder rung walking task as previously described (31). All tests were carried out blindly to the treatment. All mouse cages have been examined daily in order to determine lifespan.

Brain pathology and immunohistochemistry

WT and R6/2 mice were sacrificed by cervical dislocation. Brains were removed and trimmed by removing the olfactory bulbs and spinal cord. The remaining brain was weighed in milligrams, processed and embedded in paraffin wax, and 10 μm coronal sections were cut on an RM 2245 microtome (Leica Microsystems). Five mice/group ($n = 5$) were used, and four coronal sections spread over the anterior–posterior extent of the brain (200–300 μm inter-section distance) were scanned.

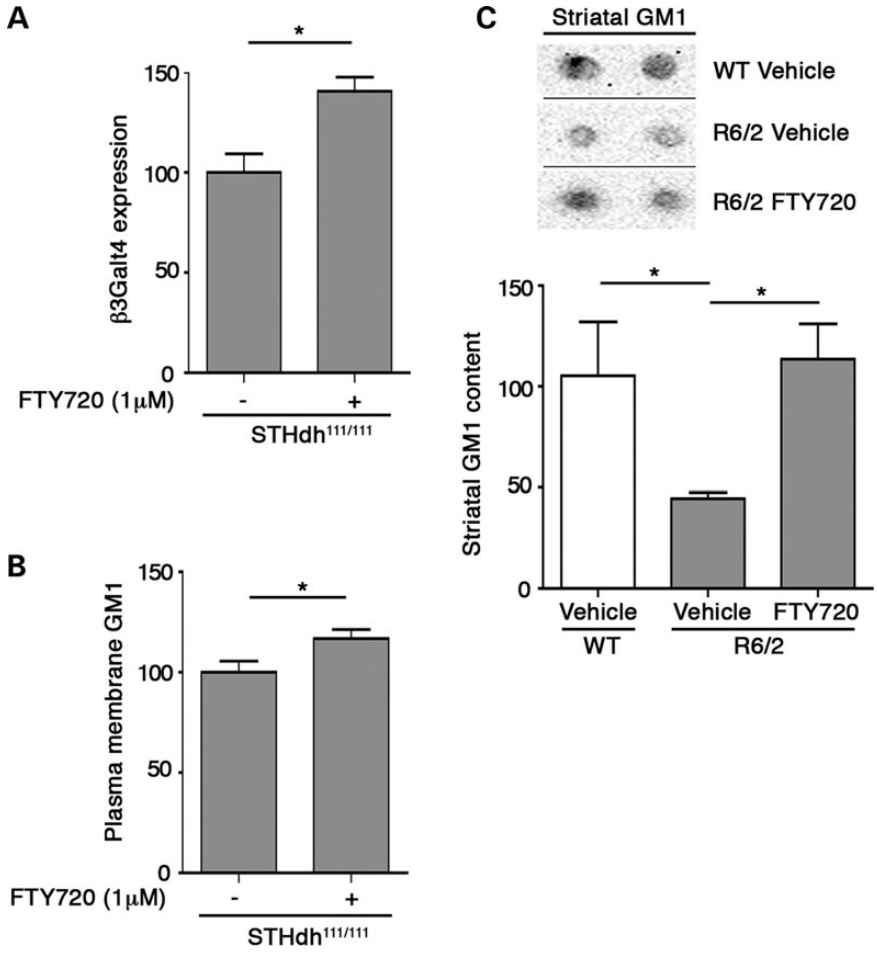

Figure 9. FTY720 increases levels of ganglioside GM1. (**A**) GM1 synthase (β3galt4) mRNA levels in STHdh$^{111/111}$ cultured for 6 h in regular medium supplemented with 1 μM FTY720. (**B**) Plasma membrane GM1 levels in STHdh$^{111/111}$ cultured for 6 days in regular medium supplemented with 1 μM FTY720. Data are represented as the mean ± SD of two experiments, each performed in quadruplicate. $^*P < 0.05$ (two-tailed test). (**C**) Representative dot-blotting and densitometric analysis of GM1 content, in striatal tissues from vehicle- and FTY720-treated mice at 11 weeks of age. Data are represented as the mean ± SD, $n = 5$ for each group of mice. $^*P < 0.05$ (non-parametric Mann–Whitney *U*-test).

For each coronal section, a total number of 10 fields at 63 × magnification were analyzed. The number of striatal cells was determined by hematoxylin/eosin staining (62). Immunostaining for mutant Htt aggregates was carried out by using EM48 antibody (1:100) (Millipore) (63). The average number and area of striatal mHtt aggregates per brain section was quantified by ImageJ software. For the analysis of CC, five animals per group were analyzed. For each coronal section, a total number of 10 fields at 5 × magnification were acquired. The thickness of CC was measured in correspondence of the middle line of the brain (Fig. 6C). All the assessments were performed blindly.

Slice preparation

Mice were anesthetized with halothane and then decapitated, and the brain rapidly removed to ice-cold glycerol-based dissection artificial cerebrospinal fluid (ACSF) containing the following (in mM): glycerol 250, KCl 2.5, $CaCl_2$ 2.4, $MgCl_2$ 1.2, NaH_2PO_4 1.2, $NaHCO_3$ 26, glucose 11 and Na-pyruvate 0.1 (pH 7.35, aerated with 95% O_2/5% CO_2, 290–300 mOsm/l). The brain was glued to the stage of a vibrating microtome (model VT1000S; Leica), and 300 μm coronal slices were cut. Slices then were stored and allowed to recover at room temperature in a submerged chamber for at least 1 h before experimentation in oxygenated standard ACSF, containing the following (in mM): NaCl 125, KCl 2.5, $CaCl_2$ 2, NaH_2PO_4 1.25, $MgCl_2$ 1, $NaHCO_3$ 26, glucose 10, Na-pyruvate 0.1 (pH 7.35, aerated with 95% O_2/5% CO_2, 290–300 mOsm/l).

Whole-cell recordings in slices

Whole-cell patch-clamp recordings were obtained from layer IV–V pyramidal cells visualized in cortical slices with the aid of infrared-differential interference contrast microscopy. The patch pipette (3–4 MΩ) was filled with the following solution (in mM): KCl 140, HEPES 10, 1,2-bis(2-aminophenoxy)ethane-*N*,*N*,*N*,*N*-tetraacetic acid 5, $MgCl_2$ 2, MgATP 2 (pH 7.35, with KOH). Voltage-clamp recordings were performed using an Axon Multiclamp 700B patch-clamp amplifier. Spontaneous inhibitory post-synaptic currents (sIPSCs) were recorded filtering

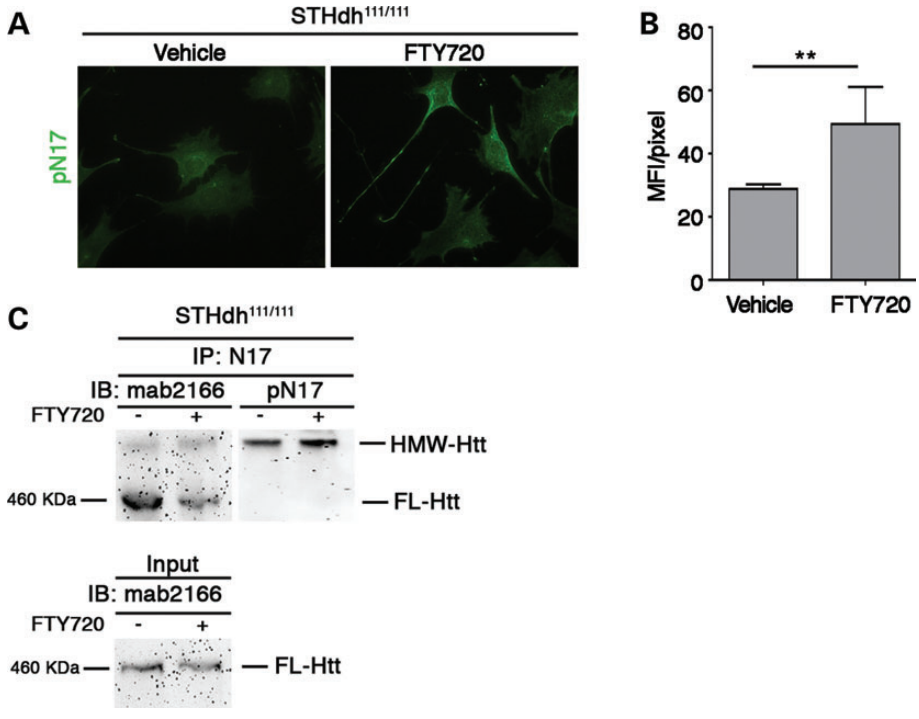

Figure 10. FTY720 induces phosphorylation of Htt at serine13/16 residues. (**A**) Representative epifluorescence microscope images. Striatal knock-in cells were incubated with either vehicle or 1 μM FTY720 for 30 min. (**B**) Graph shows pN17 immunostaining MFI per pixel ± SD, calculated over a minimum of 30 cells per experimental group. Each experiment was performed in quadruplicate. $^{*}P < 0.05$ (non-parametric Mann–Whitney *U*-test). (**C**) Analysis of mutant huntingtin phosphorylation state by immunoprecipitation and immunoblotting. Striatal knock-in cells ($STHdh^{111/111}$) were incubated with either vehicle or 1 μM FTY720 for 30 min. Mutant huntingtin was immunoprecipitated by using a rabbit polyclonal anti-huntingtin antibody (N17). Immunoprecipitated material (IP) was immunoblotted with the indicated phospho-Ser 13/16-Htt-specific antibody (pN17) and anti-huntingtin antibody (mab2166). Same amount of protein extracts were immunoprecipitated as indicated by the input lanes. HMW-Htt, high-molecular-weight huntingtin; FL-Htt, full-length huntingtin.

the membrane current at 1 kHz and digitizing at 100–200 μs, clamping cells at −70 mV, in the presence of 10 μM 6-cyano-7-nitroquinoxaline-2,3-dione (CNQX) and 50 μM DL-2-amino-5-phosphonovaleric acid (AP-5). In these conditions, synaptic currents were GABAergic in nature, as they were all blocked by 20 μM bicuculline (not shown). To record miniature currents (mIPSCs), 1 μM TTX was bath-applied to slices. All drugs were obtained from Tocris. Spontaneous synaptic currents were analyzed offline using an automatic template-based detection protocol (Clampfit 10).

RNA extraction and analysis of gene expression by real-time PCR

Total RNA were extracted using RNeasy kit (Qiagen) according to the manufacturer's instructions. One microgram of total RNA was reverse-transcribed using Superscript II reverse transcriptase (Invitrogen) and oligo-dT primer, and the resulting cDNAs were amplified using Power SYBR Green PCR Master Mix (Applied Biosystems) following the manufacturers' instructions. Quantitative PCR analysis will be performed on a StepOne instrument (Applied Biosystems) using specific primers, as reported in Supplementary Material, Table S1, as previously described (5).

Analysis of GM1 content

Plasma membrane GM1 levels were measured by cholera toxin B subunit binding and FACS analysis. Cells were cultured seven days in regular medium supplemented with 1 μM FTY720. At the end of the treatment, cells were trypsinized, washed in ice-cold PBS (Invitrogen) and labeled with 2 mg/ml Alexa488-conjugated cholera toxin B (CTX-B) (Invitrogen) in PBS/0.1% BSA for 5 min on ice. After washing, cells were fixed with 2% paraformaldehyde and stored at 4°C until FACS analysis was performed. GM1 levels in dissected mouse brain tissues were analyzed by dot-blotting as previously described (31). Striatal tissues were lysed, spotted on nitrocellulose membrane and incubated with HRP-conjugated CTX-B. Total amount of GM1 was detected by ECL Prime (GE Healthcare) and quantitated with Quantity One software (Bio-Rad Laboratories).

Htt immunoprecipitation and immunoblotting

After pre-incubation for 3 h at 33°C in serum-free medium, cells were treated with 1 μM FTY720 for 30 min and lysed in lysis buffer containing 20 mM Tris, pH 7.4, 1% Nonidet P-40, 1 mM EDTA, 20 mM NaF, 2 mM $Na3VO_4$ and 1:1000 protease inhibitor mixture (Sigma–Aldrich), sonicated with 2 × 10 s pulses and then centrifuged for 10 min at 10,000*g*. Immunoprecipitation (0.6 mg total lysate) was performed using polyclonal anti-Htt antibody N17 (31,33) complexed to protein G-Sepharose (Zymed, Invitrogen). The immunoprecipitated protein was resolved on 7% SDS–PAGE, transferred overnight on PVDF membrane (31) and detected by immunoblotting with mab2166 (1:1000) (Millipore) and anti-phospho-Ser13/16-Htt-specific antibody pN17 (1:6000) (31,33). HRP-conjugated secondary

antibodies (GE Healthcare) were used at 1:5000 dilution. Protein bands were detected by ECL Prime (GE Healthcare) and visualized by Quantity One software (Bio-Rad Laboratories).

Immunocytochemistry

Cells were grown on glass coverslips coated with 50 μg/mL poly-L-lysine and treated with either vehicle or 1 μM FTY720 for 30 min. Cells were then washed in PBS, fixed in 4% paraformaldehyde for 15 min at room temperature (RT) and permeabilized with 0.5% Triton X-100 in PBS for 5 min. After blocking with 4% donkey serum in PBS for 1 h, cells were incubated with polyclonal pN17 antibody (1:1000) for 1 h at RT. Anti-rabbit Alexa 488-conjugated secondary antibody (Vector Laboratories) was used at 1:500 dilution for 1 h at RT. Cell nuclei were stained with 4′-6 diamidino-2-phenildindole (Vector Laboratories) for 10 min at RT. Coverslips were mounted using Prolong Gold antifade reagent (Invitrogen). Images of vehicle- and FTY720-treated cells were acquired at 63× magnification using the same microscope settings. The mean fluorescence intensity (MFI) per pixel in each cell was calculated with ImageJ software (National Institutes of Health) after manual selection of cell area.

Statistics

Two-way ANOVA followed by Bonferroni post-test was used to compare treatment groups in the open field and horizontal ladder tests and for mouse body weight analysis. Non-parametric Mann–Whitey *U*-test was used to analyze cell survival, mouse brain weight, CC thickness, BDNF, DARPP-32 and MAG protein levels, mouse striatum GM1 content and cortical currents. Log-rank test was used to analyze mice survival. Two-tailed *t*-test was used to compare mean fluorescence intensity of vehicle- versus FTY720-treated samples in immunocytochemistry experiments and in all other experiments. All data are expressed as mean ± SD except in the electrophysiology studies in which data are expressed as mean ± SEM.

SUPPLEMENTARY MATERIAL

Supplementary Material is available at *HMG* online.

ACKNOWLEDGEMENTS

We thank Professor Ray Truant (McMaster University, Hamiton, ON, Canada) for providing us with pN17 and N17 antibodies. We also thank N. Panebianco and S. Sciacca for technical assistance. We gratefully acknowledge the support of Lega Italiana Ricerca Huntington (www.lirh.it) e malattie correlate onlus.

Conflict of Interest statement: none declared.

FUNDING

This research was supported by Marie Curie International Incoming Fellowship (PIIF-GA-2011-300197) granted to V.M. within the 7th European Community Framework Programme and by Telethon (Project GGP12218) to F.S.

REFERENCES

1. Novak, M.J. and Tabrizi, S.J. (2011) Huntington's disease: clinical presentation and treatment. *Int. Rev. Neurobiol.*, **98**, 297–323.
2. T.H.s.D.C.R. Group. (1993) A novel gene containing a trinucleotide repeat that is expanded and unstable on Huntington's disease chromosomes. *Cell*, **72**, 971–983.
3. Zuccato, C., Ciammola, A., Rigamonti, D., Leavitt, B.R., Goffredo, D., Conti, L., MacDonald, M.E., Friedlander, R.M., Silani, V., Hayden, M.R. *et al.* (2001) Loss of huntingtin-mediated BDNF gene transcription in Huntington's disease. *Science*, **293**, 493–498.
4. Borrell-Pages, M., Zala, D., Humbert, S. and Saudou, F. (2006) Huntington's disease: from huntingtin function and dysfunction to therapeutic strategies. *Cell. Mol. Life. Sci.*, **63**, 2642–2660.
5. Maglione, V., Marchi, P., Di Pardo, A., Lingrell, S., Horkey, M., Tidmarsh, E. and Sipione, S. (2010) Impaired ganglioside metabolism in Huntington's disease and neuroprotective role of GM1. *J. Neurosci.*, **30**, 4072–4080.
6. Chiba, K. and Adachi, K. (2012) Discovery of fingolimod, the sphingosine 1-phosphate receptor modulator and its application for the therapy of multiple sclerosis. *Future Med. Chem.*, **4**, 771–781.
7. Ali, R., Nicholas, R.S. and Muraro, P.A. (2013) Drugs in development for relapsing multiple sclerosis. *Drugs*, **73**, 625–650.
8. Spiegel, S. and Milstien, S. (2003) Exogenous and intracellularly generated sphingosine 1-phosphate can regulate cellular processes by divergent pathways. *Biochem. Soc. Trans.*, **31**, 1216–1219.
9. Brinkmann, V. (2007) Sphingosine 1-phosphate receptors in health and disease: mechanistic insights from gene deletion studies and reverse pharmacology. *Pharmacol. Ther.*, **115**, 84–105.
10. Dev, K.K., Mullershausen, F., Mattes, H., Kuhn, R.R., Bilbe, G., Hoyer, D. and Mir, A. (2008) Brain sphingosine-1-phosphate receptors: implication for FTY720 in the treatment of multiple sclerosis. *Pharmacol. Ther.*, **117**, 77–93.
11. Meno-Tetang, G.M., Li, H., Mis, S., Pyszczynski, N., Heining, P., Lowe, P. and Jusko, W.J. (2006) Physiologically based pharmacokinetic modeling of FTY720 (2-amino-2[2-(-4-octylphenyl)ethyl]propane-1,3-diol hydrochloride) in rats after oral and intravenous doses. *Drug Metab. Dispos.*, **34**, 1480–1487.
12. Billich, A., Bornancin, F., Devay, P., Mechtcheriakova, D., Urtz, N. and Baumruker, T. (2003) Phosphorylation of the immunomodulatory drug FTY720 by sphingosine kinases. *J. Biol. Chem.*, **278**, 47408–47415.
13. Brinkmann, V., Davis, M.D., Heise, C.E., Albert, R., Cottens, S., Hof, R., Bruns, C., Prieschl, E., Baumruker, T., Hiestand, P. *et al.* (2002) The immune modulator FTY720 targets sphingosine 1-phosphate receptors. *J. Biol. Chem.*, **277**, 21453–21457.
14. Miron, V.E., Schubart, A. and Antel, J.P. (2008) Central nervous system-directed effects of FTY720 (fingolimod). *J. Neurol. Sci.*, **274**, 13–17.
15. Osinde, M., Mullershausen, F. and Dev, K.K. (2007) Phosphorylated FTY720 stimulates ERK phosphorylation in astrocytes via S1P receptors. *Neuropharmacology*, **52**, 1210–1218.
16. Coelho, R.P., Payne, S.G., Bittman, R., Spiegel, S. and Sato-Bigbee, C. (2007) The immunomodulator FTY720 has a direct cytoprotective effect in oligodendrocyte progenitors. *J. Pharmacol. Exp. Ther.*, **323**, 626–635.
17. Deogracias, R., Matsumoto, T., Klein, C., Klin, C., Yazdani, M., bible, M. and Barde, Y. (2008) FTY720 induces BDNF production in neuronal cell cultures. *Neurology*, **70**, A373.
18. Di Menna, L., Molinaro, G., Di Nuzzo, L., Riozzi, B., Zappulla, C., Pozzilli, C., Turrini, R., Caraci, F., Copani, A., Battaglia, G. *et al.* (2012) Fingolimod protects cultured cortical neurons against excitotoxic death. *Pharmacol. Res.*, **67**, 1–9.
19. Deogracias, R., Yazdani, M., Dekkers, M.P., Guy, J., Ionescu, M.C., Vogt, K.E. and Barde, Y.A. (2012) Fingolimod, a sphingosine-1 phosphate receptor modulator, increases BDNF levels and improves symptoms of a mouse model of Rett syndrome. *Proc. Natl Acad. Sci. USA*, **109**, 14230–14235.
20. Bajwa, A., Jo, S.K., Ye, H., Huang, L., Dondeti, K.R., Rosin, D.L., Haase, V.H., Macdonald, T.L., Lynch, K.R. and Okusa, M.D. (2010) Activation of sphingosine-1-phosphate 1 receptor in the proximal tubule protects against ischemia-reperfusion injury. *J. Am. Soc. Nephrol.*, **21**, 955–965.
21. Stessin, A.M., Gursel, D.B., Schwartz, A., Parashar, B., Kulidzhanov, F.G., Sabbas, A.M., Boockvar, J., Nori, D. and Wernicke, A.G. (2012) FTY720, sphingosine 1-phosphate receptor modulator, selectively radioprotects hippocampal neural stem cells. *Neurosci. Lett.*, **516**, 253–258.

22. Brunati, A.M., Tibaldi, E., Carraro, A., Gringeri, E., D'Amico, F. Jr., Toninello, A., Massimino, M.L., Pagano, M.A., Nalesso, G. and Cillo, U. (2008) Cross-talk between PDGF and S1P signalling elucidates the inhibitory effect and potential antifibrotic action of the immunomodulator FTY720 in activated HSC-cultures. *Biochim. Biophys. Acta*, **1783**, 347–359.
23. Mangiarini, L., Sathasivam, K., Seller, M., Cozens, B., Harper, A., Hetherington, C., Lawton, M., Trottier, Y., Lehrach, H., Davies, S.W. *et al.* (1996) Exon 1 of the HD gene with an expanded CAG repeat is sufficient to cause a progressive neurological phenotype in transgenic mice. *Cell*, **87**, 493–506.
24. Apostol, B.L., Illes, K., Pallos, J., Bodai, L., Wu, J., Strand, A., Schweitzer, E.S., Olson, J.M., Kazantsev, A., Marsh, J.L. *et al.* (2006) Mutant huntingtin alters MAPK signaling pathways in PC12 and striatal cells: ERK1/2 protects against mutant huntingtin-associated toxicity. *Hum. Mol. Genet.*, **15**, 273–285.
25. Colin, E., Regulier, E., Perrin, V., Durr, A., Brice, A., Aebischer, P., Deglon, N., Humbert, S. and Saudou, F. (2005) Akt is altered in an animal model of Huntington's disease and in patients. *Eur. J. Neurosci.*, **21**, 1478–1488.
26. Varma, H., Yamamoto, A., Sarantos, M.R., Hughes, R.E. and Stockwell, B.R. (2010) Mutant huntingtin alters cell fate in response to microtubule depolymerization via the GEF-H1-RhoA-ERK pathway. *J. Biol. Chem.*, **285**, 37445–37457.
27. Quarles, R.H. (2007) Myelin-associated glycoprotein (MAG): past, present and beyond. *J. Neurochem.*, **100**, 1431–1448.
28. Arrasate, M. and Finkbeiner, S. (2012) Protein aggregates in Huntington's disease. *Exp. Neurol.*, **238**, 1–11.
29. Cepeda, C., Starling, A.J., Wu, N., Nguyen, O.K., Uzgil, B., Soda, T., Andre, V.M., Ariano, M.A. and Levine, M.S. (2004) Increased GABAergic function in mouse models of Huntington's disease: reversal by BDNF. *J. Neurosci. Res.*, **78**, 855–867.
30. Lahiri, S., Park, H., Laviad, E.L., Lu, X., Bittman, R. and Futerman, A.H. (2009) Ceramide synthesis is modulated by the sphingosine analog FTY720 via a mixture of uncompetitive and noncompetitive inhibition in an Acyl-CoA chain length-dependent manner. *J. Biol. Chem.*, **284**, 16090–16098.
31. Di Pardo, A., Maglione, V., Alpaugh, M., Horkey, M., Atwal, R.S., Sassone, J., Ciammola, A., Steffan, J.S., Fouad, K., Truant, R. *et al.* (2012) Ganglioside GM1 induces phosphorylation of mutant huntingtin and restores normal motor behavior in Huntington disease mice. *Proc. Natl Acad. Sci. USA*, **109**, 3528–3533.
32. Gu, X., Greiner, E.R., Mishra, R., Kodali, R., Osmand, A., Finkbeiner, S., Steffan, J.S., Thompson, L.M., Wetzel, R. and Yang, X.W. (2009) Serines 13 and 16 are critical determinants of full-length human mutant huntingtin induced disease pathogenesis in HD mice. *Neuron*, **64**, 828–840.
33. Atwal, R.S., Desmond, C.R., Caron, N., Maiuri, T., Xia, J., Sipione, S. and Truant, R. (2011) Kinase inhibitors modulate huntingtin cell localization and toxicity. *Nat. Chem. Biol.*, **7**, 453–460.
34. Suzuki, S., Enosawa, S., Kakefuda, T., Shinomiya, T., Amari, M., Naoe, S., Hoshino, Y. and Chiba, K. (1996) A novel immunosuppressant, FTY720, with a unique mechanism of action, induces long-term graft acceptance in rat and dog allotransplantation. *Transplantation*, **61**, 200–205.
35. Hemmati, F., Dargahi, L., Nasoohi, S., Omidbakhsh, R., Mohamed, Z., Chik, Z., Naidu, M. and Ahmadiani, A. (2013) Neurorestorative effect of FTY720 in a rat model of Alz'eimer's disease: Comparison with Memantine. *Behav. Brain Res.*, **252C**, 415–421.
36. Humbert, S., Bryson, E.A., Cordelieres, F.P., Connors, N.C., Datta, S.R., Finkbeiner, S., Greenberg, M.E. and Saudou, F. (2002) The IGF-1/Akt pathway is neuroprotective in Huntington's disease and involves Huntingtin phosphorylation by Akt. *Dev. Cell*, **2**, 831–837.
37. Bodai, L. and Marsh, J.L. (2012) A novel target for Huntington's disease: ERK at the crossroads of signaling. The ERK signaling pathway is implicated in Huntington's disease and its upregulation ameliorates pathology. *Bioessays*, **34**, 142–148.
38. Sarantos, M.R., Papanikolaou, T., Ellerby, L.M. and Hughes, R.E. (2012) Pizotifen activates ERK and provides neuroprotection in vitro and in vivo in models of Huntington's disease. *J. Huntingtons Dis.*, **1**, 195–210.
39. Bibb, J.A., Yan, Z., Svenningsson, P., Snyder, G.L., Pieribone, V.A., Horiuchi, A., Nairn, A.C., Messer, A. and Greengard, P. (2000) Severe deficiencies in dopamine signaling in presymptomatic Huntington's disease mice. *Proc. Natl Acad. Sci. USA*, **97**, 6809–6814.
40. Foster, C.A., Howard, L.M., Schweitzer, A., Persohn, E., Hiestand, P.C., Balatoni, B., Reuschel, R., Beerli, C., Schwartz, M. and Billich, A. (2007) Brain penetration of the oral immunomodulatory drug FTY720 and its phosphorylation in the central nervous system during experimental autoimmune encephalomyelitis: consequences for mode of action in multiple sclerosis. *J. Pharmacol. Exp. Ther.*, **323**, 469–475.
41. Kim, H.J., Miron, V.E., Dukala, D., Proia, R.L., Ludwin, S.K., Traka, M., Antel, J.P. and Soliven, B. (2011) Neurobiological effects of sphingosine 1-phosphate receptor modulation in the cuprizone model. *FASEB J.*, **25**, 1509–1518.
42. Carroll, J.B., Lerch, J.P., Franciosi, S., Spreeuw, A., Bissada, N., Henkelman, R.M. and Hayden, M.R. (2011) Natural history of disease in the YAC128 mouse reveals a discrete signature of pathology in Huntington disease. *Neurobiol. Dis.*, **43**, 257–265.
43. Xiang, Z., Valenza, M., Cui, L., Leoni, V., Jeong, H.K., Brilli, E., Zhang, J., Peng, Q., Duan, W., Reeves, S.A. *et al.* (2011) Peroxisome-proliferator-activated receptor gamma coactivator 1 alpha contributes to dysmyelination in experimental models of Huntington's disease. *J. Neurosci.*, **31**, 9544–9553.
44. Aboul-Enein, F., Rauschka, H., Kornek, B., Stadelmann, C., Stefferl, A., Bruck, W., Lucchinetti, C., Schmidbauer, M., Jellinger, K. and Lassmann, H. (2003) Preferential loss of myelin-associated glycoprotein reflects hypoxia-like white matter damage in stroke and inflammatory brain diseases. *J. Neuropathol. Exp. Neurol.*, **62**, 25–33.
45. Lopez, P.H., Ahmad, A.S., Mehta, N.R., Toner, M., Rowland, E.A., Zhang, J., Dore, S. and Schnaar, R.L. (2011) Myelin-associated glycoprotein protects neurons from excitotoxicity. *J. Neurochem.*, **116**, 900–908.
46. Nguyen, T., Mehta, N.R., Conant, K., Kim, K.J., Jones, M., Calabresi, P.A., Melli, G., Hoke, A., Schnaar, R.L., Ming, G.L. *et al.* (2009) Axonal protective effects of the myelin-associated glycoprotein. *J. Neurosci.*, **29**, 630–637.
47. Bogush, A., Pedrini, S., Pelta-Heller, J., Chan, T., Yang, Q., Mao, Z., Sluzas, E., Gieringer, T. and Ehrlich, M.E. (2007) AKT and CDK5/p35 mediate brain-derived neurotrophic factor induction of DARPP-32 in medium size spiny neurons in vitro. *J. Biol. Chem.*, **282**, 7352–7359.
48. VonDran, M.W., Singh, H., Honeywell, J.Z. and Dreyfus, C.F. (2011) Levels of BDNF impact oligodendrocyte lineage cells following a cuprizone lesion. *J. Neurosci.*, **31**, 14182–14190.
49. Binder, D.K. and Scharfman, H.E. (2004) Brain-derived neurotrophic factor. *Growth Factors*, **22**, 123–131.
50. Gauthier, L.R., Charrin, B.C., Borrell-Pages, M., Dompierre, J.P., Rangone, H., Cordelieres, F.P., De Mey, J., MacDonald, M.E., Lessmann, V., Humbert, S. *et al.* (2004) Huntingtin controls neurotrophic support and survival of neurons by enhancing BDNF vesicular transport along microtubules. *Cell*, **118**, 127–138.
51. Xie, Y., Hayden, M.R. and Xu, B. (2010) BDNF overexpression in the forebrain rescues Huntington's disease phenotypes in YAC128 mice. *J. Neurosci.*, **30**, 14708–14718.
52. Giralt, A., Carreton, O., Lao-Peregrin, C., Martin, E.D. and Alberch, J. (2011) Conditional BDNF release under pathological conditions improves Huntington's disease pathology by delaying neuronal dysfunction. *Mol. Neurodegener.*, **6**, 71.
53. Cummings, D.M., Andre, V.M., Uzgil, B.O., Gee, S.M., Fisher, Y.E., Cepeda, C. and Levine, M.S. (2009) Alterations in cortical excitation and inhibition in genetic mouse models of Huntington's disease. *J. Neurosci.*, **29**, 10371–10386.
54. Arrasate, M., Mitra, S., Schweitzer, E.S., Segal, M.R. and Finkbeiner, S. (2004) Inclusion body formation reduces levels of mutant huntingtin and the risk of neuronal death. *Nature*, **431**, 805–810.
55. Sanchez, I., Mahlke, C. and Yuan, J. (2003) Pivotal role of oligomerization in expanded polyglutamine neurodegenerative disorders. *Nature*, **421**, 373–379.
56. Payne, S.G., Oskeritzian, C.A., Griffiths, R., Subramanian, P., Barbour, S.E., Chalfant, C.E., Milstien, S. and Spiegel, S. (2007) The immunosuppressant drug FTY720 inhibits cytosolic phospholipase A2 independently of sphingosine-1-phosphate receptors. *Blood*, **109**, 1077–1785.
57. Caron, N.S., Desmond, C.R., Xia, J. and Truant, R. (2013) Polyglutamine domain flexibility mediates the proximity between flanking sequences in huntingtin. *Proc. Natl Acad. Sci. USA*, **110**, 14610–14615.

58. Mishra, R., Hoop, C.L., Kodali, R., Sahoo, B., van der Wel, P.C. and Wetzel, R. (2012) Serine phosphorylation suppresses huntingtin amyloid accumulation by altering protein aggregation properties. *J. Mol. Biol.*, **424**, 1–14.
59. Thompson, L.M., Aiken, C.T., Kaltenbach, L.S., Agrawal, N., Illes, K., Khoshnan, A., Martinez-Vincente, M., Arrasate, M., O'Rourke, J.G., Khashwji, H. *et al.* (2009) IKK phosphorylates Huntingtin and targets it for degradation by the proteasome and lysosome. *J. Cell. Biol.*, **187**, 1083–1099.
60. Benn, C.L., Landles, C., Li, H., Strand, A.D., Woodman, B., Sathasivam, K., Li, S.H., Ghazi-Noori, S., Hockly, E., Faruque, S.M. *et al.* (2005) Contribution of nuclear and extranuclear polyQ to neurological phenotypes in mouse models of Huntington's disease. *Hum. Mol. Genet.*, **14**, 3065–3078.
61. Ontaneda, D., Hara-Cleaver, C., Rudick, R.A., Cohen, J.A. and Bermel, R.A. (2012) Early tolerability and safety of fingolimod in clinical practice. *J. Neurol. Sci.*, **323**, 167–172.
62. Bancroft, G.J. and Gamble, M. (2008) *Theory and Using Fresh Solutions. Regarding H&E Staining, Formalin Pigment Practice of Histological Techniques*. Churchill Livingstone, Edinburgh.
63. Li, H., Li, S.H., Yu, Z.X., Shelbourne, P. and Li, X.J. (2001) Huntingtin aggregate-associated axonal degeneration is an early pathological event in Huntington's disease mice. *J. Neurosci.*, **21**, 8473–8481.